PHYSICAL REVIEW B **73**, 052504 (2006)

Structural distortion and suppression of superconductivity in stoichiometric *B*1-MoN epitaxial thin films

Kei Inumaru, Kazuya Baba, and Shoji Yamanaka
Department of Applied Chemistry, Hiroshima University, 1-4-1, Kagamiyama, Higashi-Hiroshima 739-8527, Hiroshima, Japan
(Received 10 October 2005; published 16 February 2006)

Molybdenum nitride films with the NaCl structure (*B*1-MoN) were epitaxially grown on α-Al_2O_3(001) and MgO(001) substrates at 973 K by pulsed laser deposition (PLD) under nitrogen radical irradiation. The highly crystalline epitaxial films enabled us to determine the three-dimensional cell parameters, which was motivated by theoretical calculations that *B*1-MoN, a predicted superconductor, is elastically unstable against tetragonal and trigonal distortions. On α-Al_2O_3(001), the *B*1-MoN phase (composition, $Mo_1N_{0.98}$) was grown with its (111) planes parallel to the substrate surface. X-ray diffraction analysis with a multiaxes diffractometer detected only a small trigonal lattice distortion [a=0.4219(3) nm, α=89.28(5)°] with an expansion along the [111] direction perpendicular to the substrate surface. The film grown on MgO(001) had the $MoN_{1.03}$ composition and showed a slight tetragonal distortion (a=0.4213 and c=0.424 nm) due to fitting to the MgO substrate lattice (a=0.4213 nm). These two stoichiometric films showed no superconductivity above 2 K. A lower nitrogen content ($MoN_{0.86}$) film was obtained on α-Al_2O_3(001) using a higher deposition rate. The corresponding film had a much smaller lattice constant [a=0.4184(3) nm], and a similar distortion [α=89.41(5)°]. The *B*1-$MoN_{0.86}$ film showed superconductivity with a transition temperature T_c=4.2 K. The suppression of the superconductivity of the former stoichiometric phase can be interpreted in terms of the lattice expansion.

DOI: 10.1103/PhysRevB.73.052504 PACS number(s): 74.78.−w, 81.15.Fg

Molybdenum nitrides have attracted much attention as superconducting materials. Molybdenum forms several crystalline nitrides including γ-Mo_2N (cubic), β-Mo_2N (tetragonal), and hexagonal δ-MoN.[1,2] γ-Mo_2N is known as a superconductor with $T_c \sim 5$ K.[3] We reported that β-Mo_2N is also a superconductor with $T_c \sim 5$ K.[4] It was reported that the hexagonal δ-MoN was crystallized in a slightly distorted NiAs type structure under 6 GPa,[5,6] and the resulting phase showed superconductivity with $T_c \sim 12$ K.[3,5] A theoretical study predicted that MoN with the cubic NaCl type structure (so called *B*1-MoN) would have T_c as high as 29 K.[7–10] Since *B*1-MoN is believed to be a metastable phase, many studies adopted thin film deposition techniques, such as magnetron sputter, ion-beam assisted deposition, and ion implanting for the synthesis of the phase.[11–17] The *B*1-MoN films reported in the literature, however, have not exhibited such "high T_c." Later, theoretical studies predicted the elastic instability of the *B*1-MoN cubic structure, and suggested that orthorhombic, tetragonal or trigonal distortions would be more preferable.[18,19] Therefore, lattice distortion as well as chemical composition should be analysed at the same time to confirm the formation of *B*1-MoN. However, to our knowledge, no study reported three-dimensional lattice parameters for the *B*1-MoN thin films. This is probably due to the difficulty in obtaining highly crystalline *B*1-MoN films, and the difficulty in determining the cell parameters of oriented thin films by x-ray diffraction.

Here, we report the preparation and characterization of well-crystallized *B*1-MoN films epitaxially grown on α-Al_2O_3(001) and MgO(001) substrates by PLD under nitrogen radical irradiation. Their three-dimensional lattice parameters were determined by x-ray diffraction with a multiaxes diffractometer and high-resolution reciprocal space mapping of x-ray diffraction. Superconductivity of the films is discussed in relation to the lattice distortion, the chemical composition, and the lattice expansion.

The PLD system used in this study was equipped with a KrF excimer laser (COMPex102, Lambda Physics, Goettingen, Germany) and an rf-plasma radical source (model rf4.5, SVTA, MN, USA). The residual pressure of the chamber was less than 10^{-8} Torr. A Mo disk (99.9%) was used as the target. The oxide substrates were cleaned in methanol before their introduction into the vacuum chamber. Nitride films were deposited under irradiation of nitrogen radicals [rf power 350 W, N_2 feed 0.5 cm^3 (STP)/min]. We previously reported highly crystalline TiN,[20] CrN,[21] TiN-CrN multilayers,[22] Sr_2N,[23] and $Ti_{1-x}Ni_xN_y$ (Ref. 24) films prepared under radical irradiation. Recently, highly crystalline epitaxial CrN films were prepared by a similar technique.[25] In this study, we adopted a substrate temperature as high as 973 K to obtain highly crystalline films. As is mentioned later, high nitrogen contents were achieved for the films even at high substrate temperatures, which may be due to the high reactivity of the nitrogen radical beam. The pulse repetition rate was 20 Hz. Deposition rate was controlled by changing the power of the laser pulses (80–300 mJ). We found that the nitrogen content could be well controlled by changing the growth rates of the films, and that stoichiometric films (Mo/N molar ratio=1) could be obtained at very low growth rates.[26] Deposition conditions for the films denoted by A, B, and C are listed in Table I. The crystal structures of the films were characterized by x-ray diffraction using two diffractometers. Conventional $\omega-2\theta$ scans were performed with an M18FHX diffractometer (MacScience, Tokyo) using Cu $K\alpha$ radiation. Pole figure measurements, $\omega-2\theta$ scans at variant Ψ angles, and x-ray diffraction reciprocal space mapping

TABLE I. Deposition conditions, structural parameters, and other properties for $B1$-MoN thin films. T_s, substrate temperature; r_{av}, average deposition rate; t_f, film thickness.

Sample	Substrate	T_s (K)	r_{av} (nm h^{-1})	t_f (nm)	x in MoNx	Cell parameters a (nm)	c (nm)	α (°)	T_c (K)
Film A	α-Al_2O_3(001)	973	2.7	30	0.98	0.4219(3)[a]	---	89.28(5)[a]	<2
Film B	α-Al_2O_3(001)	973	8.2	49	0.86	0.4184(3)[a]	---	89.41(5)[a]	4.2
Film C	MgO(001)	1023	4.6	27	1.03	0.4213[b]	0.424[b]	90	<2
γ-Mo_2N					0.5[c]	0.4163[c]		90[c]	5[d]

[a]Refined on the basis of multiaxes x-ray diffraction data. See the text.
[b]Determined by x-ray reciprocal space mapping.
[c]ICSD 76281; PDF card 251366.
[d]Ref. 3.

were carried out with an XPert MRD diffractometer (Philips). The incident beam was a Cu $K\alpha$ parallel beam from an x-ray mirror with a crossed slit (0.5 mm width and 5 mm height). The detector was equipped with a parallel-plate collimator and a Graphite monochromator (resolution, 0.27°). For the reciprocal space mapping, Ge-crystal monochromators were used in the incident x-ray generation (divergence 0.003°) and detection (acceptance angle 0.005°). The nitrogen contents in the films were determined with an x-ray photoelectron spectrometer, which was calibrated with a standard γ-Mo_2N powder sample. Magnetic measurements were carried out with an MPMS-5S magnetometer (Quantum Design, USA). The thin film was placed parallel to the applied magnetic field. Film thickness was measured by AFM with a Nanoscope D-3100 (Digital Instrument, USA) operated in tapping mode.

Figure 1 shows x-ray diffraction patterns (conventional $\omega-2\theta$ scan) of the $B1$-MoN films grown at different growth rates on α-Al_2O_3(001). The deposition conditions are listed in Table I. For the sample deposited at a low growth rate (film A), an intense peak was observed at $2\theta=36.46°$ that could be assigned to $B1$-MoN(111). For the sample deposited at a higher growth rate (film B), the diffraction peak shifted to a higher angle ($2\theta=36.97°$), indicating the shrinking of the lattice in the film. In order to obtain more information on the lattice constants, diffraction peaks from crystal planes not parallel to the substrate surface were measured using the diffractometer equipped with a multiaxes sample stage. For films A and B, 111, 200, 220, and 113 diffractions were measured at optimized positions, and the obtained d values were used to calculate the cell parameters. The results are listed in Table I.

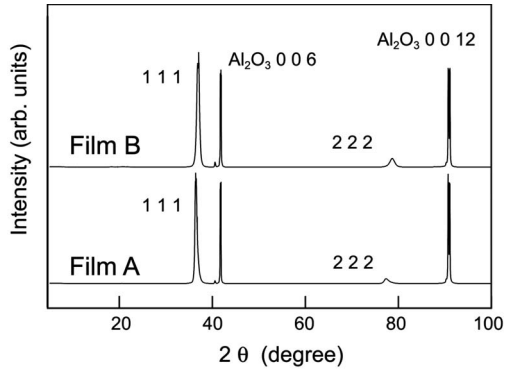

FIG. 1. X-ray diffraction patterns of epitaxial $B1$-MoN films on α-Al_2O_3(001).

For the film grown on MgO(001) (film C), the x-ray diffraction reciprocal space mapping was carried out to determine the cell parameters. In the map of film C (not shown), the $B1$-MoN 113 signal was observed just below the MgO 113 spot, demonstrating that the lattice constant a of the film became identical to that of MgO (0.4213 nm) as a result of the epitaxy. The lattice constants were determined from the map to be $a=0.4213$ and $c=0.424$ nm with a small tetragonal distortion ($c/a=1.006$).

Compositions of the films were determined by x-ray photoelectron spectroscopy. Peaks of N1s and Mo $3p_{3/2}$ were separated by subtraction of a Mo $3p_{3/2}$ signal obtained from a measurement of Mo metal foil. A bulk γ-Mo_2N, of composition $Mo_1N_{0.43}$, as determined by chemical analysis, was used as a standard to calibrate the x-ray photoelectron spectrometer.[26] The results were listed in Table I. Films A and C were stoichiometric $B1$-MoN. Sample B, which was deposited at a higher rate, had a lower nitrogen composition $Mo_1N_{0.86}$.

Figure 2 shows the temperature dependence of the magnetic susceptibility. The strong diamagnetism demonstrated that the sample B was superconducting below 4.2 K. On the other hand, films A and C showed no superconductivity above 2 K. Since both films A and B were grown on α-Al_2O_3(001), the comparison between them would highlight the factors influential to the superconductivity. Theoretical calculations predicted the elastic instability of bulk cubic $B1$-MoN. According to the calculation by Chen *et al.*,[18] $B1$-MoN has a total energy minimum at around 8% trigonal distortion, which correspond to the cell parameter $\alpha=80.6°$. In the present study, the stoichiometric and nitrogen-deficient $B1$-MoN films (A and B) had a much smaller distortion of $\alpha=89.3-89.4°$. We cannot estimate what extent the thin films can be considered "bulklike" in terms of elastic instability. For epitaxial CrN films (thickness ~150 nm) on MgO,

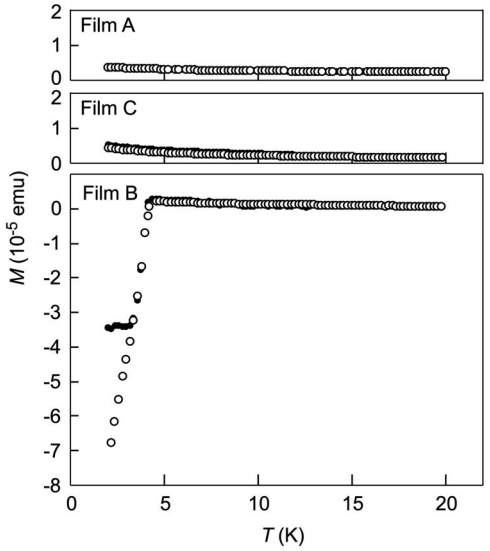

FIG. 2. Temperature dependence of magnetic moment for $B1$ -MoN films. Open and solid circles represent zero-field cooling and field cooling, respectively. Magnetic field, 20 Oe.

it was reported that a transition was observed at a temperature similar to that for bulk CrN structural (and magnetic) transition.[25] The important fact here is that the lattice distortions in the present MoN films were small. It is possible that the α-$Al_2O_3(001)$ substrate binds the $B1$-MoN crystalline films to the surface and suppresses the large distortion expected for the bulk MoN crystal. In spite of the small difference in α between samples A and B, the lattice constants a were very different for these two films: The stoichiometric film $MoN_{0.98}$ (film A) had a much larger lattice constant a [0.4219(3) nm] than the nitrogen-deficient film MoN0.86 [film B, $a=0.4184(3)$ nm]. Therefore, the increase in nitrogen content and/or cell expansion appeared to be factors strongly influential to the superconductivity rather than the crystal distortions. In other words, the nitrogen deficient $B1$ -MoN showed superconductivity and the increase in nitrogen to the stoichiometric composition, accompanied by cell expansion, suppressed the superconductivity. The $B1$-MoN film grown on MgO (film C) was also consistent with the results for film A: Film C had a stoichiometric composition $Mo_1N_{1.03}$. This sample had a small tetragonal distortion due to the epitaxy to fit the film lattice to the substrate MgO lattice ($a=0.4213$ nm). The cell constant c was as large as 0.4240 nm, and the cell volume was 75.26×10^{-3} nm^3, which is comparable to that for film A (75.08×10^{-3} nm^3) and is much larger than that for sample B (73.23×10^{-3} nm^3). The film C showed no superconductivity above 2 K, consistent with the results for film A.

Our observation is qualitatively consistent with the report by Linker *et al.*[11] The authors prepared polycrystalline MoN films by reactive magnetron sputtering at 773 K or below. They observed that the superconductivity of Mo_1N_x ($T_c=3$ K when $x=1$) was suppressed as x increased from 1 to around 1.2. They reported that the increase of the substrate temperature up to 973 K brought about a significant lattice shrinking due to decomposition of the nitride. Our pulsed laser deposition under the nitrogen radical irradiation was able to give stoichiometric $B1$-MoN at substrate temperature as high as 973 K. Thus, this method gave well-crystallized epitaxial $B1$-MoN films, and the lattice distortion could be analyzed precisely. We could change the nitrogen content by changing the deposition rate. Although the cell distortion was small ($\alpha=89.3°-89.4°$) and seemed to be independent on the nitrogen contents, the lattice constant a was highly dependent on the nitrogen contents: The increase in nitrogen from $Mo_1N_{0.86}$ to $Mo_1N_{0.98}$ brought about the lattice expansion from $a=0.4184(3)$ to 0.4219(3) nm. Considering that the lattice constant a of γ-Mo_2N is reported to be 0.4163 nm, the value changed very steeply between films A and B with unknown reasons. One possibility is the change in the site occupation: For example, nitrogen begins to occupy interstitial sites at the nearly stoichiometric composition. However, the x-ray photoelectron spectroscopy could not detect the meaningful difference in the state of nitrogen between films A and B: N $1s_{1/2}$ positions were almost the same for films A and B (397.4 and 397.5 eV, respectively). The peak positions (Table II) gave some information on the nature of the chemical bond between Mo and N: The N$1s_{1/2}$ signal for the $B1$ -MoN films appeared at a position close to that of a covalent nitride Si_3N_4 rather than that of a isoelectronic CrN, where Cr belongs to the same group (group 6) in the periodic table of elements as Mo. These results showed that the bonds between Mo and N were more covalent than the Cr-N bonds in CrN.

TABLE II. Comparison of x-ray photoelectron spectra binding energies.

	Binding energy (eV)			
Sample	Mo $3d_{3/2}$	Mo $3d_{5/2}$	Mo $3p_{3/2}$	N $1s_{1/2}$
Film A	231.1	227.9	394.0	397.4
Film B	231.0	228.0	394.1	397.6
Film C	231.4	228.2	394.2	397.5
Mo (metal)[a]		227.85		
Mo_2C[a]		227.8		
MoB_2[a]		227.9		
MoO_3[a]		232.8		
CrN[a]				396.8
Si_3N_4[a]				397.7
BN[a]				398.1

[a]*Practical Surface Analysis*, 2nd ed., edited by D. Briggs and M. P. Seah (Wiley, New York, 1990), Vol. 1, p. 599.

In conclusion, we could prepare well-crystallized stoichiometric and nitrogen-deficient $B1$-MoN films by pulsed laser deposition, and their three-dimensional cell parameters were determined by x-ray diffraction. Irrespective of theoretical calculations that bulk $B1$-MoN is elastically unstable against trigonal and tetragonal distortion, the crystal distortion in the films was small. The nitrogen deficient $B1$-MoN ($MoN_{0.86}$) film showed superconductivity up to 4.2 K. The increase in nitrogen to the stoichiometric composition, and

the accompanying cell expansion, suppressed the superconductivity. The steep cell expansion observed between the nitrogen deficient films and the stoichiometric films may be related to the observed suppression of superconductivity and needs further investigation.

This work was partially supported by a COE project and a Grant-in-Aid from the Japan Ministry of Education for Science, Culture, Sports and Technology (MEXT), and a CREST project from the Japan Science and Technology Corporation (JST).

[1] H. Jehn and P. Ettmayer, J. Less-Common Met. **58**, 85 (1978).
[2] P. Ettmayer, Monatsch. Chem. **101**, 127 (1970).
[3] B. T. Matthias and J. K. Hulm, Phys. Rev. **87**, 799 (1952).
[4] K. Inumaru, K. Baba, and S. Yamanaka, Chem. Mater. **17**, 5935 (2005).
[5] C. L. Bull, P. F. McMillan, E. Soignard, and K. Leinenweber, J. Solid State Chem. **177**, 1488 (2004).
[6] A. Bezinge, K. Yvon, and J. Muller, Solid State Commun. **63**, 141 (1987).
[7] W. E. Pickett, B. M. Klein, and D. A. Papaconstantopoulos, Physica B **107**, 667 (1981).
[8] D. A. Papaconstantopoulos, W. E. Pickett, B. M. Klein, and L. L. Boyer, Nature (London) **308**, 494 (1984).
[9] D. A. Papaconstantopoulos, W. E. Pickett, E. M. Klein, and L. L. Boyer, Phys. Rev. B **31**, 752 (1985).
[10] D. A. Papaconstantopoulos and W. E. Pickett, Phys. Rev. B **31**, 7093 (1985).
[11] G. Linker, R. Smithey, and O. Meyer, J. Phys. F: Met. Phys. **14**, L115 (1984).
[12] H. Yamamoto, T. Miki, and M. Tanaka, Adv. Cryog. Eng. **32**, 671 (1986).
[13] N. Terada, M. Nose, and Y. Hoshi, Adv. Cryog. Eng. **32**, 663 (1986).
[14] K. Saito and Y. Asada, J. Phys. F: Met. Phys. **17**, 2273 (1987).
[15] H. Ihara, Y. Kimura, K. Senzaki, H. Kezuka, and M. Hirabayashi, Phys. Rev. B **31**, 3177 (1985).
[16] H. Ihara, M. Hirabayashi, K. Senzaki, Y. Kimura, and H. Kezuka, Phys. Rev. B **32**, 1816 (1985).
[17] N. Savvides, J. Appl. Phys. **62**, 600 (1987).
[18] J. Chen, H. Krakauer, and M. J. Mehl, Phys. Rev. B **37**, 3295 (1988).
[19] G. L. W. Hart and B. M. Klein, Phys. Rev. B **61**, 3151 (2000).
[20] K. Inumaru, T. Ohara, and S. Yamanaka, Appl. Surf. Sci. **158**, 375 (2000).
[21] K. Inumaru, H. Okamoto, and S. Yamanaka, J. Cryst. Growth **237**, 2050 (2002).
[22] K. Inumaru, T. Ohara, K. Tanaka, and S. Yamanaka, Appl. Surf. Sci. **235**, 460 (2004).
[23] K. Inumaru, Y. Kuroda, K. Sakamoto, M. Murashima, and S. Yamanaka, J. Alloys Compd. **372**, L1 (2004).
[24] K. Sakamoto, K. Inumaru, and S. Yamanaka, Appl. Surf. Sci. **199**, 303 (2002).
[25] C. Constantin, B. Muhammad, D. Ingram, and A. R. Smith, Appl. Phys. Lett. **85**, 671 (2004).
[26] K. Inumaru, K. Baba, and S. Yamanaka, Physica B (to be published).